



## Electrospun nanofibrous biodegradable polyester coatings on Bioglass<sup>®</sup>-based glass-ceramics for tissue engineering

Oana Bretcanu<sup>a</sup>, Superb K. Misra<sup>a</sup>, D. Mohammad Yunos<sup>a</sup>, Aldo R. Boccaccini<sup>a,\*</sup>, Ipsita Roy<sup>b</sup>, Tomasz Kowalczyk<sup>c</sup>, Slawomir Blonski<sup>c</sup>, Tomasz A. Kowalewski<sup>c</sup>

<sup>a</sup> Department of Materials, Imperial College London, UK

<sup>b</sup> Department of Molecular and Applied Biosciences, University of Westminster, UK

<sup>c</sup> Institute of Fundamental Technology Research Polish Academy of Sciences (IPPT PAN), Warsaw, Poland

### ARTICLE INFO

#### Article history:

Received 23 February 2009

Received in revised form 16 July 2009

Accepted 11 August 2009

#### Keywords:

Electrospinning

Nanofibers

Bioglass<sup>®</sup>

Polyhydroxyalkanoates

Tissue engineering

### ABSTRACT

Biodegradable polymeric nanofibrous coatings were obtained by electrospinning different polymers onto sintered 45S5 Bioglass<sup>®</sup>-based glass-ceramic pellets. The investigated polymers were poly(3-hydroxybutyrate) (P3HB), poly(3-hydroxybutyrate-co-hydroxyvalerate) (PHBV) and a composite of poly(caprolactone) (PCL) and poly(ethylene oxide) (PEO) (PCL-PEO). The fibrous coatings morphology was evaluated by optical microscopy and scanning electron microscopy. The electrospinning process parameters were optimised to obtain reproducible coatings formed by a thin web of polymer nanofibers. *In-vitro* studies in simulated body fluid (SBF) were performed to investigate the bioactivity and mineralisation of the substrates by inducing the formation of hydroxyapatite (HA) on the nanofiber-coated pellets. HA crystals were detected on all samples after 7 days of immersion in SBF, however the morphology of the HA layer depended on the characteristic fibre diameter, which in turn was a function of the specific polymer-solvent system used. The bioactive and resorbable nanofibrous coatings can be used to tailor the surface topography of bioactive glass-ceramics for applications in tissue engineering scaffolds.

© 2009 Elsevier B.V. All rights reserved.

### 1. Introduction

Electrospinning is a process that produces ultrafine polymer fibres of diameters ranging from tens of micrometers down to several nanometers [1–6]. One of the major application fields of electrospinning is the biomedical materials sector [7], where electrospun fibrous structures have been proposed as substrates and scaffolds for artificial tissue and organ regeneration [8] as well as for drug encapsulation and release [9]. Many synthetic and natural polymers have been used for electrospinning. Polyesters (e.g., PDLLA, PLGA, PCL) are a very common group of polymers used to construct biodegradable nanofibrous materials for tissue engineering scaffolds [6,7]. Poly(3-hydroxybutyrate) (P3HB), a polymer which can be obtained by biosynthesis from bacteria [10,11], is another biodegradable polymer currently investigated for scaffold development using electrospinning [12,13].

Tissue engineering strategies require a biodegradable scaffold as the substrate and structural matrix for cell attachment and proliferation [14]. It is generally agreed that highly porous microstructures with large surface area stimulate cell growth.

For bone regeneration, for example, pore sizes of at least 100 μm and interconnected 3D pore structures with porosity >80% are required [15]. Biodegradable and biocompatible polyester nanofibers obtained by electrospinning seem to be well suited to generate highly porous microstructures for scaffold application [13,16], however electrospun nanofibrous scaffolds lack the ability to produce the required 3D macroporous geometry. In addition electrospun nanofibrous structures do not exhibit sufficient mechanical competence required for scaffolds intended for bone tissue engineering [17].

Bioactive ceramics and glasses are attractive materials for bone replacement and bone engineering [18]. These materials, however, are brittle and exhibit low fracture strength, in particular when fabricated in porous form [19]. Moreover, using pure inorganic materials makes difficult the encapsulation of drugs or growth factors that promote cells adhesion and proliferation due to the high temperatures involved in their processing, e.g., 1100 °C in the case of glass-ceramic scaffolds [20]. Alternative materials for bone tissue engineering scaffolds are composites formed by the combination of biodegradable polymers and bioactive inorganic particles [21]. Recently, for example, a new family of biocomposites made of P3HB containing Bioglass<sup>®</sup> particles has been developed and demonstrated to be promising materials for bone implants and tissue engineering scaffolds, as a bone-like hydroxyapatite layer

\* Corresponding author.

E-mail address: [a.boccaccini@imperial.ac.uk](mailto:a.boccaccini@imperial.ac.uk) (A.R. Boccaccini).

could be formed on the scaffold surface in contact with simulated body fluid (SBF) [22]. Moreover bioresorbable and bioactive polymer/Bioglass® composites with tailored pore structure and glass-ceramic scaffolds coated with biodegradable polymer layers have already been tested for bone tissue engineering applications [23,24]. The combination of biodegradable polymer (electrospun) nanofibres and Bioglass®-based scaffolds, however, has not been investigated to date. There is interest in incorporating a fibrous (nano)topography on the surface of the bioactive glass substrate to mimic the structure of the natural extracellular matrix (ECM), which cannot be achieved by the free bioactive glass surface. Thus the aim of the present work is to develop bioresorbable nanofibrous coatings on Bioglass®-derived glass-ceramic substrates to mimic the architecture of the ECM. In addition, we hypothesized that combination of electrospun polymer nanofibres and bioactive glass-ceramic scaffolds will enable: (i) the ordered formation of nanostructured hydroxyapatite (mineralisation) upon contact of the material with physiological fluids (e.g., SBF), which is of significance to achieve strong bonding to new bone tissue, and (ii) the addition of a controllable drug delivery function to the scaffold, e.g., making possible the loading of biomolecules into the polymer fibres [9] and using the bioactive glass-ceramic substrate as the structure carrier.

To the best of our knowledge, we present here the first approach which combines electrospinning of polymeric nanofibres and bioactive glass-ceramics by producing a biodegradable nanofibrous web covering the surface of Bioglass®-based substrates. The ultimate goal is to fabricate a bioactive composite material featuring a surface fibrous nanotopography which, upon mineralisation in contact with relevant fluids, e.g., SBF, will mimic the local architecture of the bone ECM for tissue engineering applications. The biomaterials bioactivity and mineralisation were assessed using an acellular SBF. The polymers used were poly(3-hydroxybutyrate) (P3HB) and poly(3-hydroxybutyrate-co-3-hydroxyvalerate) (PHBV), a copolymer of almost identical structure to P3HB but of mechanical properties improved by the presence of less stiff valerate units. Another material, tested for comparison, was poly(caprolactone) (PCL), which is a well known polymer for biomedical applications [6]. The electrospinning of this last material was facilitated by the addition of another biodegradable polymer, poly(ethylene oxide) (PEO), which is extensively used in electrospinning [1,2,25].

## 2. Experimental

### 2.1. Materials

The commercial materials used were PEO of molecular weight  $4 \times 10^5$  Da (Aldrich), PCL of Mn = 65,000 Da (Aldrich), 2,2,2-trifluoroethanol (TFE) (Alfa Aesar) and chloroform (POCH). All commercial compounds and solvents were of analytical purity and were used as received without further purification. Poly(3-hydroxybutyrate) (P3HB) (molecular weight 398,000) was purchased from Fluka Chemicals (Schnellendorf, Germany) and used without further purification. Poly(3-hydroxybutyrate-co-3-hydroxyvalerate) (PHBV) containing 2% hydroxyvalerate was purchased from Goodfellow.

To prepare polymer solutions suitable for electrospinning, P3HB and PHBV were dissolved in TFE. The solutions were heated for 2 min at 60 °C to speed up the dissolution process and then cooled to room temperature. The preparation of composite PCL-PEO material was as follows: PEO (1.25 wt%) was dissolved in chloroform, heated to 50 °C in a closed vial and left overnight to cool down. Afterwards PCL (1.25 wt%) was added and the solution was left for one additional hour at room temperature to achieve complete dissolution. The PCL-PEO 50:50 mass ratio was chosen for production of a polymer leaching system that would create nano-cavities in each PCL nanofibre, although this particular aspect was not investigated in detail in the present study, as it has been considered elsewhere [26].

### 2.2. Bioactive glass-ceramic substrate preparation

Bioactive glass-ceramic substrates were fabricated using the processing parameters optimised previously for fabrication of 3D scaffolds from 45S5 Bioglass® powder by the foam replica technique [20]. The substrates in the form of flat

discs were produced by pressing Bioglass® powder followed by sintering. Briefly, commercially available 45S5 Bioglass® powder with mean particle size  $<5 \mu\text{m}$  (NovaMin USA), was pressed in cylindrical moulds (diameter = 10 mm) using a uniaxial hydraulic press. The obtained discs were sintered at 1100 °C for 1 h (heating rate  $5^\circ\text{C min}^{-1}$ ). As reported in the literature [20], this sintering heat treatment of 45S5 Bioglass® leads to densification by viscous flow and crystallization of  $\text{Na}_2\text{Ca}_2\text{Si}_3\text{O}_9$  as main crystalline phase. The sintered pellets were polished with SiC abrasive paper up to 1200 grit and used as the target substrate in the electrospinning process.

### 2.3. Electrospinning equipment

The experimental setup was composed of a high voltage power supply based on DC to DC converter (EMCO 4330) and a sensitive amplifier (nanoampere range), which was used to measure the electric current carried by the electrospun nanofibers. The setup permitted remote voltage adjustment in the range 0–33 kV with maximum current output 0.3 mA. A syringe pump (Ascor S.A., AP12) was used to maintain a constant volume flow rate of the polymer solution. A high speed CMOS camera (PCO Imaging, pco.1200hs) was used to observe and record the electrospinning process.

### 2.4. Electrospinning process

The electrospinning process involves elongation of a liquid jet in an electrostatic field. The bending instability and the consequential looping motion of the jet results in a high drawing ratio and ultra thin fibres are produced and collected on a ground electrode. Electrospinning of the tested polymers was performed as described in detail by Kowalewski et al. [27,28]. Briefly, the process was realized in a chamber of approximately  $1 \text{ m}^3$  volume. The spinneret was made of a 2 mm long flat grounded syringe needle with 0.35 mm internal diameter mounted vertically on an electrically insulated stand. The spinneret needle was attached to the positive outlet of a high voltage power supply and connected through PTFE tubing to a plastic syringe filled with the spinning solution. A constant volume flow rate was maintained using the syringe pump. The pump electronics was protected by the grounded anti-discharge cage made of wire. A flat cooper grid (310 mm  $\times$  240 mm) equipped with a small copper wire cage (75 mm  $\times$  80 mm  $\times$  50 mm) served as ground electrode. The Bioglass® pellets were positioned on microscope cover glass slides (0.1 mm  $\times$  24 mm  $\times$  60 mm, Roth, Karlsruhe) that were placed on the copper cage. The pellets were one-side coated with a thin layer of the nanofibres web. The coated pellets were first inspected by using an optical microscope to optimise the coating layer (e.g., by a trial-and-error approach). After several tests the optimal spinneret-target distance was set to 15 cm, and the variables used for the electrospinning optimisation were limited to applied voltage, concentration of polymer blend in solution and flow rate. The experiments were conducted at room temperature (usually 25–30 °C) and ambient humidity of 30–50%.

### 2.5. Characterisation and bioactivity tests

An epi-fluorescence microscope (Nikon, Eclipse E-50i) equipped with high resolution CCD camera (Bassler, A102f) was used to characterise optical characteristics of nanofibers.

The bioactivity and mineralisation test was carried out using the standard acellular in-vitro procedure described by Kokubo et al. [29]. The nanofiber-coated pellets were immersed in 10 ml of acellular simulated body fluid (pH 7.30 at 37 °C) in conical flasks. The conical flasks were placed in an incubator at 37 °C. The SBF solution was refreshed twice a week. The samples were removed from the SBF solution after 1, 3, 7 and 14 days. After being removed from the SBF fluid, the samples were gently rinsed with deionised water and left to dry in desiccators at room temperature.

The surface morphology of the incubated samples was observed by SEM (FEI-SEM LEO1535). Samples were gold coated and examined at an accelerating voltage of 15–20 kV. X-ray diffraction (XRD) patterns of the coated samples before and after soaking in SBF were registered by a Philips diffractometer using  $\text{Cu K}\alpha$  radiation in the range 15–70° ( $2\theta$ ) at 40 kV and 40 mA. The hydroxyapatite phase identification was performed by "X'Pert HighScore" program, using the PCPDFWIN database.

## 3. Results and discussion

The electrospinning process allows production of nanofibers from a large number of natural and artificial polymers or their blends [1–6]. However, finding proper conditions for a stable process is very laborious. Several regimes of the process can be observed by varying key parameters, starting with liquid dripping from the nozzle, through the electro-spraying and irregular jet-like ejections, until the periodic looping motion of the jet is established. The voltage applied between the spinneret and the target, the spinneret–nozzle distance, the feed rate of the pump, and the properties of the electrospinning solution (e.g., viscosity, viscoelasticity, conductivity, surface tension, dielectric properties, volatility

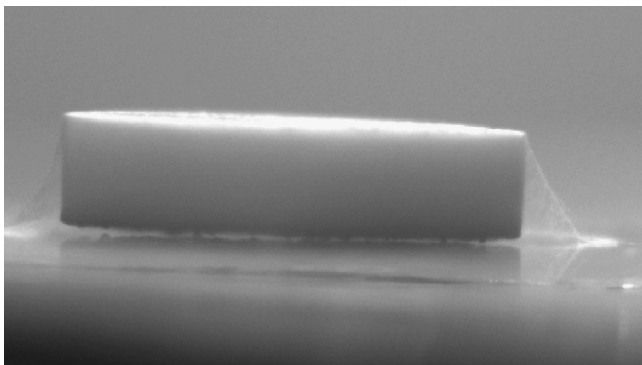


**Fig. 1.** PHB nanofibres web covering the surface of the Bioglass® pellet. Picture width: 6.9 mm.

of the solvent), together with the polymer solution properties (chain length, polydispersity, chain entanglement) themselves, and the external parameters (humidity, temperature, concentration of solvent vapour), are parameters known to affect the electrospinning process. In addition, the initial perturbations of the flow rate or the induced electric charge are responsible for possible irregularities in the amplitude of the electrospinning looping motion. Such perturbations usually result in the formation of nanofibers with “beads”, the most common of the structural defects found in electrospinning [25].

Finding the optimal configuration of electrospinning begins with the preparation of the polymer solution. For example, for

P3HB and PHBV it was found that the use of heated chloroform is a technically unreliable method. Hence 2,2,2-trifluoroethanol, typically used for dissolving proteins or polar compounds, was used in the present experiment. We found that this solvent provides very stable electrospinning conditions and produces reproducible nanofibrous structures over a broad range of polymer concentrations, applied voltages and external conditions. A digital photo image of a Bioglass®-derived pellet one-side coated with a web of electrospun P3HB nanofibres is shown in Fig. 1. A SEM micrograph of a P3HB nanofibre coated sample is shown in Fig. 2. The images show the collected nanofibers with only a small amount of “beads on string” defects.

To obtain nanoporous structures experiments with a two-polymer composite system consisting of PEO (soluble in water) and PCL (insoluble in water) were also conducted. The 50:50 mass ratio chosen for production of this composite polymer was aimed at creating a polymer leaching system that would induce formation of nano-cavities in each PCL nanofiber, which, in the case of bone tissue engineering applications, should promote osteoblast adhesion and proliferation. The use of a two-polymer blend could potentially create problems with the design of nanofibrous drug delivery structures, but the system was considered relevant in this investigation to test the possibility of constructing such a system for tissue engineering scaffolds with nanofibrous surface roughness. SEM images of PCL-PEO nanofibre coated glass-ceramic pellets obtained using different flow rates are shown in Fig. 3. Using an optimised flow rate of  $0.5 \text{ cc h}^{-1}$ , no polymeric droplets are visible (Fig. 3a). However, for the higher flow rate of  $1 \text{ cc h}^{-1}$ , many polymeric droplets are obtained on the sample surface (Fig. 3b).

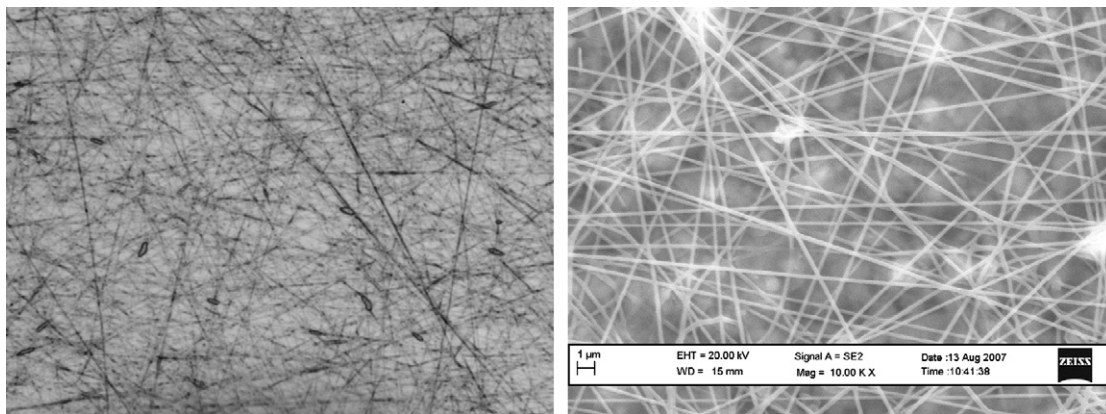


**Fig. 2.** PHB nanofibres observed in the optical microscope (left, picture width 0.18 mm), and in the SEM (right). Both pictures show a little amount of fiber defects (“beads”).

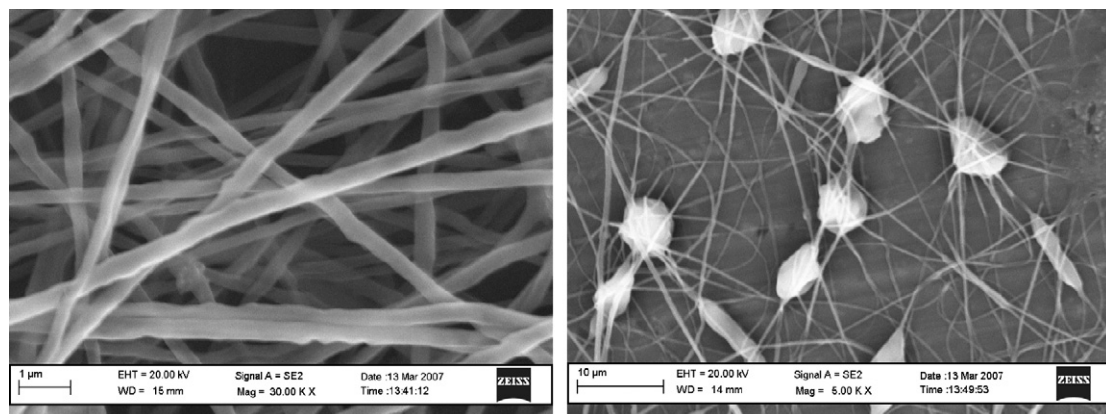


**Fig. 3.** Optimisation of electrospinning process: SEM picture of nanofibres made of poly(ethylene oxide)-poly(caprolactone) 50%:50% composite produced at different flow rates. Left – optimal flow rate  $0.5 \text{ cc h}^{-1}$ , right – non-optimal flow rate  $1 \text{ cc h}^{-1}$ , polymer droplets visible.

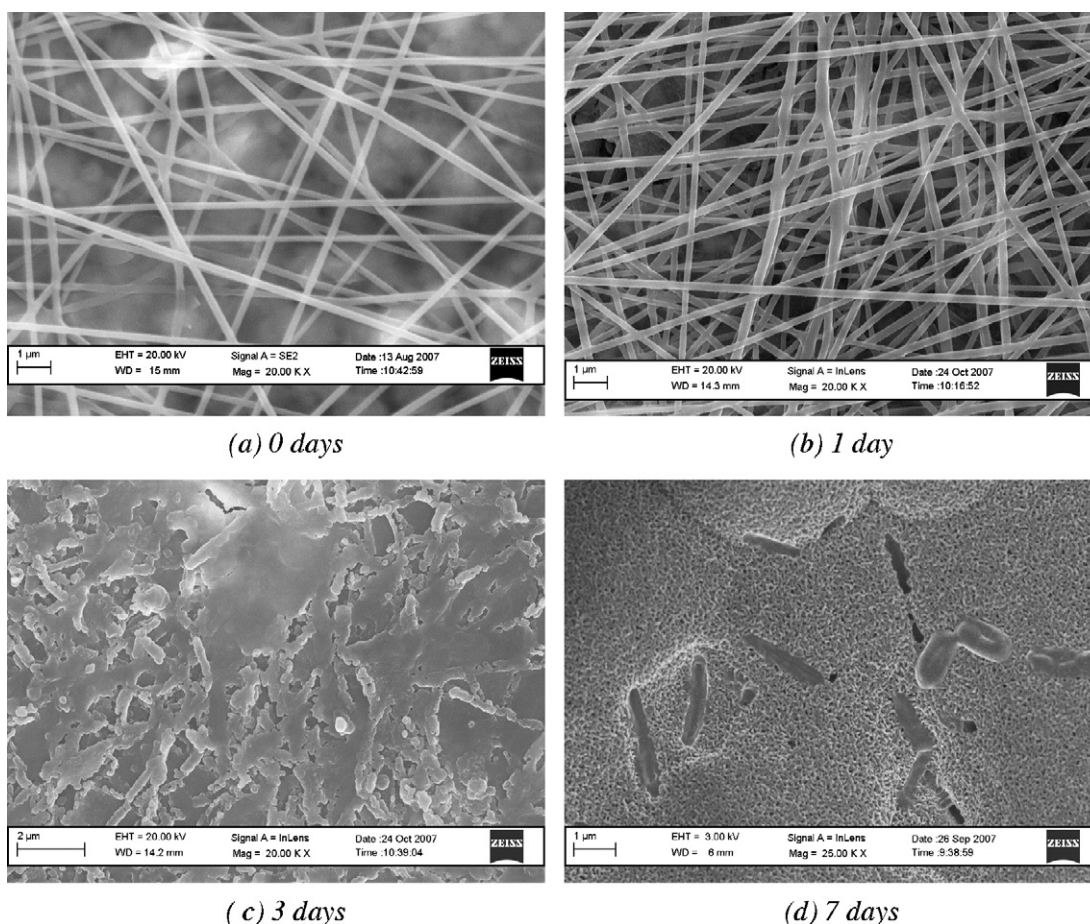


**Fig. 4.** PHB nanofibrous coating on Bioglass<sup>®</sup> pellet immersed in SBF for the specified numbers of days. At day 1, there is no visible changes when compared with the starting sample, while at 3 days the structure seems to be degraded or hydrolyzed, however it still maintains a fibrous structure. After 7 days of immersion in SBF, the surface has lost the fibrous morphology and it is fully covered with hydroxyapatite crystals.

Figs. 4–8 show the results of the SEM and XRD investigations on nanofibrous web coated Bioglass<sup>®</sup>-based glass-ceramic substrates before and after immersion in SBF, for P3HB (Figs. 4 and 5), PHBV (Fig. 6) and PCL-PEO (Figs. 7 and 8). Both the P3HB (Fig. 4) and PHBV (Fig. 6) fibres obtained from TFE solutions were thinner (typical diameter 100 nm) than PCL-PEO (Fig. 7) composite nanofibers prepared from chloroform solution (typical diameter 600 nm). It appears that the geometry of the nanofibrous material is markedly affected by the type of the polymer and solvent selected.

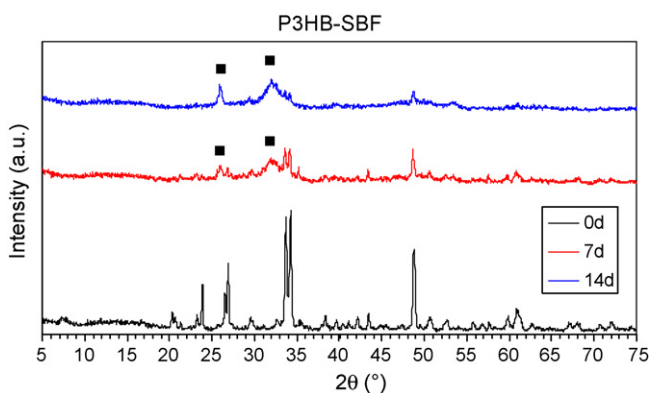


**Fig. 5.** XRD pattern of a Bioglass<sup>®</sup> based sintered glass-ceramic pellet covered with PHB nanofibres after immersion in a SBF for the specified numbers of days. The hydroxyapatite peaks, marked with (■) are present both after 7 and 14 days.

The treatment of the materials in SBF was carried out to investigate the biomineralisation process, which is assessed by the formation of hydroxyapatite on the fibrous topography assisted by the chemical reactions between the bioactive glass-ceramic surface and SBF, as described below. It should be pointed out that biomineralisation of fibrous substrates formed by electrospinning by immersion in SBF and in related fluids has been shown in several studies, as reviewed by Martins et al. [30]. For example, the mineralisation of electrospun PCL nanofibres has been demonstrated by biomimetic calcium phosphate coating using a surface treatment with solutions containing calcium and phosphate ions and by subsequent immersion in concentrated SBF [31]. In the present study, the formation of crystalline hydroxyapatite (HA) on specimen surfaces confirms that the nanofibrous coatings do not impair the bioactive behaviour of the Bioglass<sup>®</sup> substrates. After 7 days in SBF, for example, SEM observation (Fig. 4) demonstrated that the surface of a P3HA nanofibre coated substrate was completely covered with HA crystals, the initial fibrous coating is no longer visible. The X-ray diffraction patterns (Fig. 5) confirm the formation of hydroxyapatite crystals within 7 days of immersion in SBF. The formation of HA on the surface of Bioglass<sup>®</sup> and glass-ceramics in contact with SBF has been investigated by several researchers since this HA formation is used as the marker to assess the bioactivity of the materials indicating the degree of biomineralisation [18]. It is well known that in the sequence of reactions on the surface of Bioglass<sup>®</sup> in contact with SBF, the silicate network first dissolves to form a silica-gel layer; then an amorphous calcium phosphate is formed from the hydrated silica-gel; and finally apatite crystallites

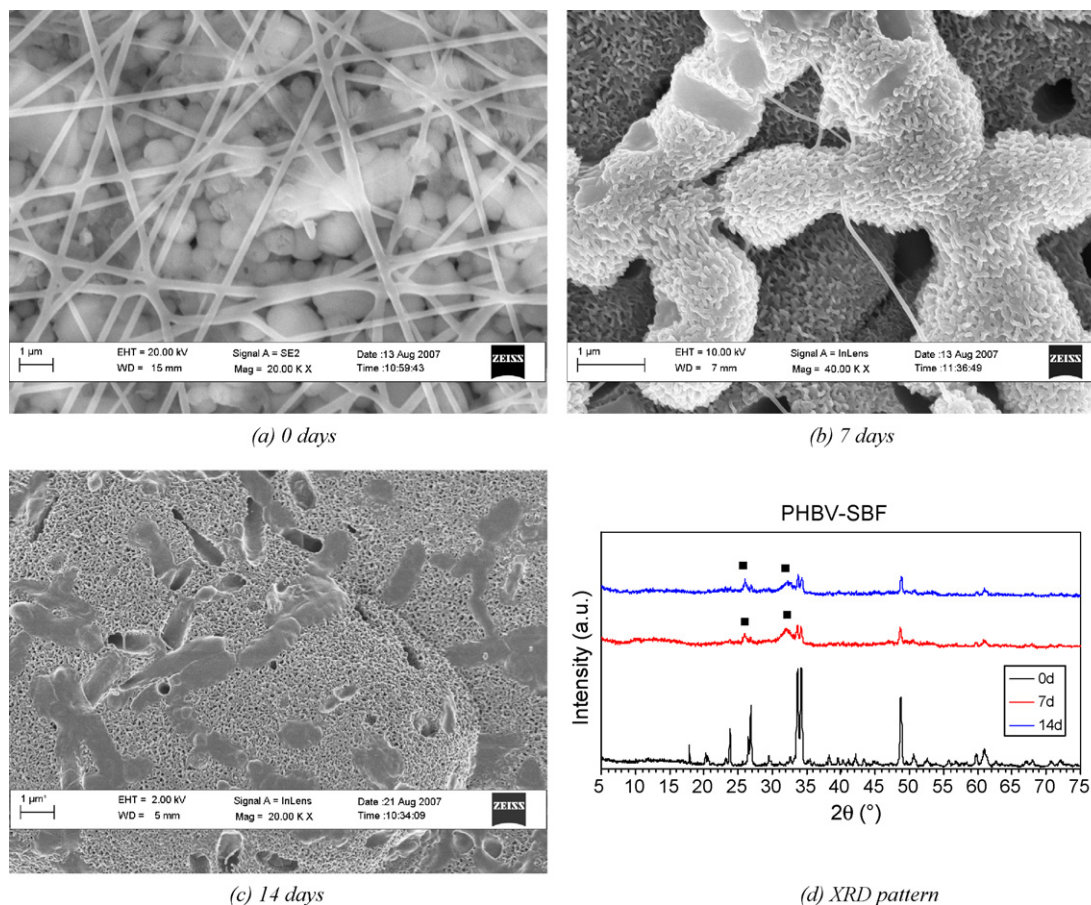


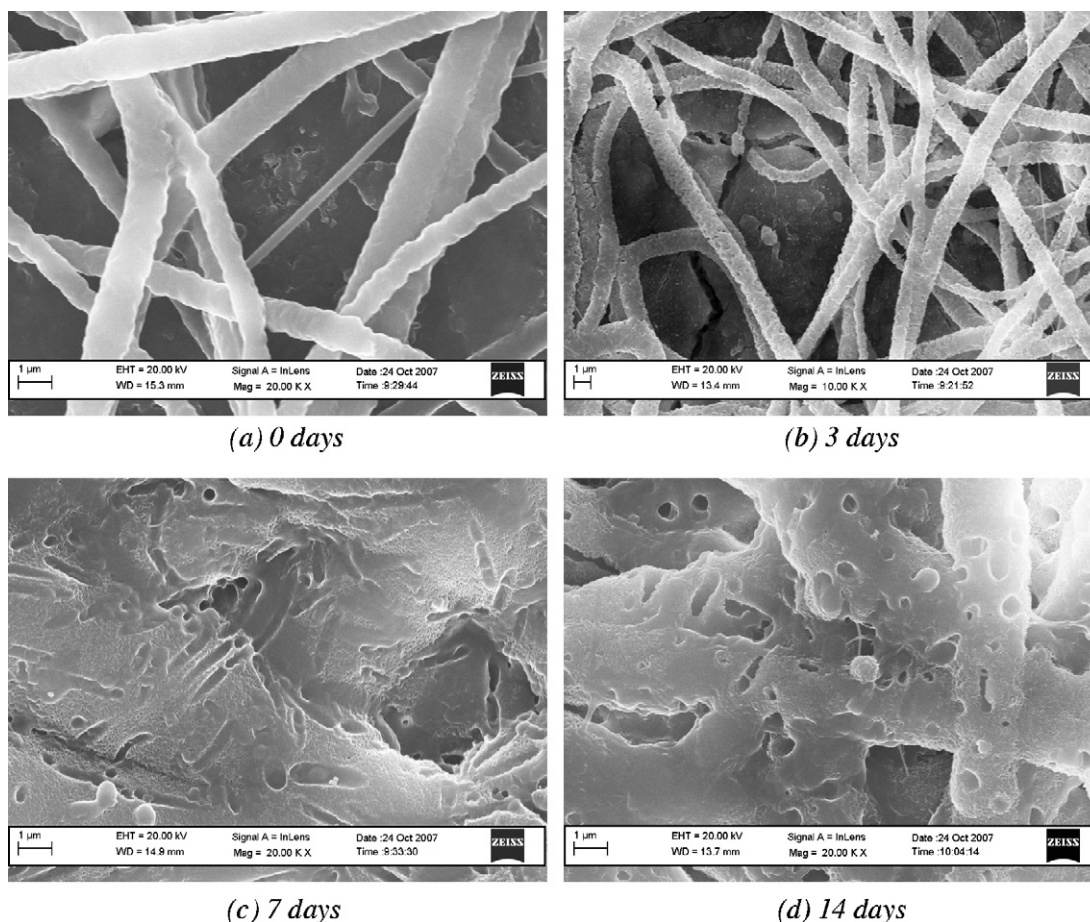
**Fig. 6.** PHBV nanofibrous coating on Bioglass<sup>®</sup> pellet immersed in SBF for the specified numbers of days. After 7 days the sample is coated by hydroxyapatite crystals, but the presence of a fibrous structure remains. At 14 days the sample is completely coated by hydroxyapatite. The XRD pattern shows the hydroxyapatite peaks, marked with (■) present both after 7 and 14 days.

nucleate and grow from the amorphous calcium phosphate [18]. It has been also shown that this reaction sequence is applicable to  $\text{Na}_2\text{Ca}_2\text{Si}_3\text{O}_9$  crystallites as well [20], confirming the bioactivity of the Bioglass<sup>®</sup>-derived glass-ceramics investigated here.

The PHBV nanofiber coating (Fig. 6) showed similar features when compared with P3HB fibres (Fig. 4) and the surface bioactivity, measured by the extent of formation of HA, seems qualitatively to remain at the same level. As can be seen in Fig. 6, the X-ray diffraction patterns of PHBV showed similar pattern of HA formation when compared with P3HB, indicating the presence of crystalline HA.

The appearance of glass-ceramic substrates coated with PCL-PEO composite fibres seems to be somewhat different in terms of surface morphology when compared with that of P3HB and PHBV composites. Fig. 7a indicates that, in average, the diameter of PCL-PEO fibres is larger than that of other fibres made from P3HB and PHBV (Figs. 4a and 6a, respectively). The composite PCL-PEO fibres were obtained using a different solvent (chloroform vs. TFE) and the composition of the polymers was different (50% polyether PEO vs. 100% polyester), resulting in almost five times thicker fibres. However the bioactivity of the composites, in terms of HA formation in contact with SBF, is qualitatively similar to that of the previous composites. It is interesting to note that after only 3 days of immersion in SBF, surface cracks characteristics of a dried silica-gel layer are present. Inspecting a typical SEM image at this time point (Fig. 7b), it is possible to observe the presence of fibres without HA nanocrystals coating. The SEM images obtained after 7 and 14 days of immersion in SBF, on the other hand (Fig. 7c and d, respectively), show that a uniform layer of HA reproducing the morphology of the original fibrous coat-

ing has been deposited. The X-ray diffraction patterns of PCL-PEO coatings indicate the characteristics peaks corresponding to HA crystals after 7 and 14 days of immersion in SBF (Fig. 8). The present results indicate that for the conditions of the present experiments, where the polymer fibres were directly deposited on a highly bioactive substrate, it is difficult to reproduce the fibrous structure by the coated HA crystals with fibres of diameter in the nanometer range (e.g., for P3HB and PHBV fibres in this case). When thicker fibres were considered, e.g., PCL-PEO fibres, the formation of HA layers follow the topography presented by the fibrous substrate. There has been considerable research in the literature with varying degree of success aiming at the biomineralisation of electrospun polymer fibrous substrates by immersion in different fluids or by special treatment of the fibre surfaces [30–33]. Differences found in the rate and morphology of the apatite formation have been attributed to the surface functional groups on the polymer nanofibres [33]. For example, when using a natural fibre such as collagen, the large number of negatively charged carboxyl and carbonyl chemical groups that can readily bind  $\text{Ca}^{2+}$  are considered to be responsibly for the high rate of nucleation of apatite crystals during mineralisation. On the other hand very low extent of hydroxyapatite formation has been detected on electrospun PLGA nanofibres tested under similar conditions [33], which has been ascribed to the less availability of surface chemical groups in PLGA (in comparison to collagen) for chelating calcium ions at the initial stage of mineralisation. Moreover the formation of apatite was seen to be non-uniform on the finest PLGA nanofibres, and no mineralisation was induced on fibres of larger diameter (e.g., 320 nm) due to the lower surface area associated with thicker fibres. The results of



(a) 0 days

(b) 3 days

(c) 7 days

(d) 14 days

**Fig. 7.** SEM images of a PCL-PEO composite fibrous coating on Bioglass<sup>®</sup> sintered pellet after immersion in SBF for the specified number of days. After 3 and 7 days the fibrous structure is maintained, also new nanoporous features are visible. After 14 days of immersion in SBF nanoporosity and nanobridges are present.

our study should demonstrate that mineralisation of thicker fibres, such as the PCL-PEO fibres developed here (Fig. 7c and d) is possible in the presence of a bioactive surface, such as bioactive glass-ceramic, which induces the mineralisation process. Similar results were achieved by Araujo et al. [31], who induced the mineralisation of electrospun PCL nanofibre meshes by biomimetic calcium phosphate coating using a surface treatment with solutions containing calcium and phosphate ions and subsequent immersion in SBF with nearly 1.5 times the ionic concentration of human blood plasma.

Alternatives investigated to induce the mineralisation of nanofibrous structures include the use of composite fibres in which the bioactive component, e.g., HA nanoparticles, are encapsulated in the electrospun polymer (PCL) nanofibres [34]. The influence of the bone-like apatite layer on the viability, adhesion and proliferation of human osteoblast-like cells has been positively assessed in mineralised PCL substrates [31], which indicates that the present nanofibrous coated Bioglass<sup>®</sup> derived glass-ceramics with HA coatings are suitable substrates for bone tissue engineering applications. Future work should focus therefore on the development of nanofibre coated 3D porous Bioglass<sup>®</sup> scaffolds.

#### 4. Conclusions

Electrospun nanofibers obtained from P(3HB), PHBV and PCL-PEO were deposited on Bioglass<sup>®</sup>-based glass-ceramic substrates and the bioactivity and mineralisation potential of the coated substrates was tested by immersion in SBF. It was found that all samples are highly bioactive and promote hydroxyapatite crystal growth on their surfaces after 7 days of immersion in SBF. However differences were found regarding the morphology of the fibres and the resultant hydroxyapatite coating layer. Only in thicker fibres, e.g., PCL-PEO fibres of 600 nm diameter, the fibrous structure could be retained after immersion in SBF for 14 days. The strategy of combining bioactive glass-ceramic surfaces with electrospun nanofibrous coating to provide mineralised nanofibrous substrates for bone tissue engineering should thus be optimised in terms of fibre size and SBF treatment. The formation of hydroxyapatite crystals on nanofibrous surfaces provides a suit-

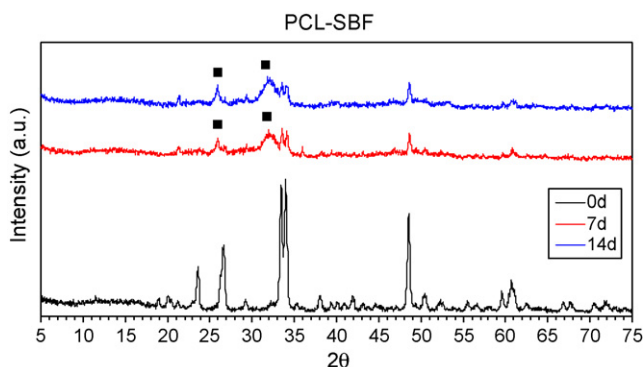


**Fig. 8.** XRD patterns obtained on a Bioglass<sup>®</sup> based sintered glass-ceramic pellet coated with PCL-PEO composite fibres, after immersion in a SBF for the specified numbers of days. The hydroxyapatite peaks, marked with (■) are present both after 7 and 14 days.

able topography mimicking the extra cellular matrix which should enhance osteoblast cell attachment and proliferation, this being the focus of current investigations.

### Acknowledgements

This work was partly supported by the Polish Ministry of Science (grant N508 031 31/1740). The authors acknowledge also financial support from the EU via the Marie Curie fellowship scheme (grant MEIF-CT-2005-024248).

### References

- [1] Ch. Burger, B.S. Hsiao, B. Chu, *Annual Review Materials Research* 36 (2006) 333.
- [2] D.H. Reneker, A.L. Yarin, E. Zussman, H. Xu, *Advances in Applied Mechanics* 41 (2007) 43.
- [3] A. Greiner, J.H. Wendorff, A.L. Yarin, E. Zussman, *Applied Microbiology and Biotechnology* 71 (2006) 387–393.
- [4] Y. Dror, W. Salalha, R. Avrahami, E. Zussman, A.L. Yarin, R. Dersch, A. Greiner, J.H. Wendorff, *Small* 3 (2007) 1064–1073.
- [5] A.L. Yarin, E. Zussman, J.H. Wendorff, A. Greiner, *Journal of Materials Chemistry* 17 (2007) 2585–2599.
- [6] Y.Z. Zhang, X. Wang, Y. Feng, J. Li, C.T. Lim, S. Ramakrishna, *Biomacromolecules* 7 (2006) 1049–1057.
- [7] Y.Z. Zhang, J. Venugopal, Z.M. Huang, C.T. Lim, S. Ramakrishna, *Biomacromolecules* 6 (2005) 2583–2589.
- [8] S. Arumuganathar, S.N. Jayashinghe, *Biomacromolecules* 9 (2008) 759–766.
- [9] M. Song, Ch. Pan, Ch. Chen, J. Li, X. Wang, Z. Gu, *Applied Surface Science* 255 (2008) 610–612.
- [10] A.G. Mikos, A.J. Thorsen, L.A. Czerwonka, Y. Bao, R. Langer, D.N. Winslow, J.P. Vacanti, *Polymer* 35 (1994) 1068–1077.
- [11] S.P. Valappil, D. Peiris, G.J. Langley, J.M. Herniman, A.R. Boccaccini, C. Bucke, I. Roy, *Journal of Biotechnology* 127 (2007) 475–487.
- [12] Y. Hu, D.W. Grainger, S.R. Winn, J.O. Hollinger, *Journal of Biomedical Materials Research* 59 (2002) 563–572.
- [13] W.-J. Li, R.M. Shanti, R.S. Tuan, *Electrospinning technology for nanofibrous scaffolds in tissue engineering*, in: S.S.R. Kumar Challa (Ed.), *Nanotechnologies for the Life Sciences*, vol. 9, Wiley-VCH, Weinheim, 2006, pp. 135–187 (Chapter 3).
- [14] D.W. Hutmacher, *Scaffolds in tissue engineering bone and cartilage*, *Biomaterials* 21 (2000) 2529–2543.
- [15] A.R. Boccaccini, V. Maquet, *Composites Science and Technology* 63 (2003) 2417–2429.
- [16] H. Yoshimoto, Y.M. Shin, H. Terai, J.P. Vacanti, *Biomaterials* 24 (2003) 2077–2082.
- [17] A. Martins, R.L. Reis, N.M. Neves, *Electrospinning: processing technique for tissue engineering scaffolding*, *International Material Reviews* 53 (2008) 257–274.
- [18] L.L. Hench, *Bioceramics*, *Journal of the American Ceramic Society* 81 (1998) 1705–1728.
- [19] O. Bretcanu, Q. Chen, S.K. Misra, A.R. Boccaccini, I. Roy, E. Verne, C.V. Brovarone, *European Journal of Glass Science and Technology – Part A* 48 (2007) 227–234.
- [20] Q.Z. Chen, I.D. Thompson, A.R. Boccaccini, *Biomaterials* 27 (2006) 2414–2425.
- [21] K. Rezwani, Q.Z. Chen, J.J. Blaker, A.R. Boccaccini, *Biomaterials* 27 (2006) 3413–3431.
- [22] S.K. Misra, D. Mohn, T.J. Brunner, W.J. Stark, S.E. Philip, I. Roy, V. Salih, J.C. Knowles, A.R. Boccaccini, *Biomaterials* 29 (2008) 1750–1761.
- [23] J.A. Roether, J.E. Gough, A.R. Boccaccini, L.L. Hench, V. Maquet, R. Jerome, *Journal of Material Science: Materials in Medicine* 13 (2002) 1207–1214.
- [24] O. Bretcanu, S. Bretcanu, I. Roy, C. Renghini, F. Fiori, A.R. Boccaccini, V.J. Salih, *Journal of Tissue Engineering and Regenerative Medicine* 3 (2009) 139–148.
- [25] S. Tripatanasuwan, Z. Zhong, D.H. Reneker, *Polymer* 48 (2007) 5742–5746.
- [26] D. Kolbuk, P. Sajkiewicz, T.A. Kowalewski, *Proceedings of International Conference on Nano and Micromechanics*, Krasiczyn, 8–10 July, 2008, p. 107.
- [27] T.A. Kowalewski, S. Barral, T. Kowalczyk, *IUTAM Symposium on Modelling Nanomaterials and Nanosystems*, Aalborg, Denmark, May 2008, IUTAM Book-series, vol. 13, Springer Science+Business Media B.V., 2009, pp. 279–293.
- [28] T.A. Kowalewski, S. Blonski, S. Barral, *Bulletin of the Polish Academy of Science: Technical Sciences* 53 (2005) 385–394.
- [29] T. Kokubo, H. Kushitani, S. Sakka, T. Kitsugi, T. Yamamuro, *Journal of Material Research* 24 (1990) 721–734.
- [30] A. Martins, R.L. Reis, N.M. Neves, *International Material Reviews* 53 (2008) 257–274.
- [31] J.V. Araujo, A. Martins, I.B. Leonor, E.D. Pinho, R.L. Reis, N.M. Neves, *Journal of Biomaterials Science. Polymer Edition* 19 (2008) 1261–1278.
- [32] S. Liao, W. Wang, M. Uo, S. Ohkawa, T. Akasaka, K. Tamura, F. Cui, F. Watari, *Biomaterials* 26 (2005) 7564–7571.
- [33] S. Liao, R. Murugan, C.K. Chan, S. Ramakrishna, *Journal of the Mechanical Behaviour of Biomedical Materials* 1 (2008) 252–260.
- [34] P. Wutticharoenmongkol, N. Sanchavanakit, P. Pavasant, P. Supaphol, *Macromolecular Bioscience* 6 (2006) 70–77.